

Oxygen vacancy induced room temperature ferromagnetism in $(\text{In}_{1-x}\text{Ni}_x)_2\text{O}_3$ thin films

D Chakraborty¹, S Kaleemulla^{2*}, M Kuppan^{2,3}, N M Rao⁴, C Krishnamoorthi⁵, I Omkaram⁶, D S Reddy⁷ and G V Rao⁸

¹Department of Physics, School of Advanced Sciences, VIT, Vellore, Tamil Nadu 632 014, India

²Thin Films Laboratory, Center for Crystal Growth, VIT, Vellore, Tamil Nadu 632 014, India

³Center for Regional Revitalization in Research and Education of Akita University, Akita University, Akita City 010-8502, Japan

⁴Department of Physics, VIT-AP, Amaravati, Andhra Pradesh 522237, India

⁵Center for Nanotechnology Research, VIT, Vellore, Tamil Nadu 632 014, India

⁶School of Advanced Materials Sciences and Engineering, Sungkyunkwan University, Gyeonggi 16419, Republic of Korea

⁷Department of Physics and Sungkyunkwan Advanced Institute of Nanotechnology (SAINT), Sungkyunkwan University, Suwon 440-746, Republic of Korea

⁸Materials Physics Division, Indira Gandhi Centre for Atomic Research, Kalpakkam, Tamil Nadu 603102, India

Received: 11 April 2017 / Accepted: 26 September 2017 / Published online: 15 December 2017

Abstract: Nickel doped indium oxide thin films $(\text{In}_{1-x}\text{Ni}_x)_2\text{O}_3$ at $x = 0.00, 0.03, 0.05$ and 0.07 were deposited onto glass substrates by electron beam evaporation technique. The deposited thin films were subjected to annealing in air at 250°C , 350°C and 450°C for 2 h using high temperature furnace. A set of films were vacuum annealed at 450°C to study the role of oxygen on magnetic properties of the $(\text{In}_{1-x}\text{Ni}_x)_2\text{O}_3$ thin films. The thin films were subjected to different characterization techniques to study their structural, chemical, surface, optical and magnetic properties. All the synthesized air annealed and vacuum annealed films exhibit body centered cubic structure without any secondary phases. No significant change in the diffraction peak position, either to lower or higher diffraction angles has been observed. The band gap of the films decreased from 3.73 eV to 3.63 eV with increase of annealing temperature from 250°C to 450°C , in the presence of air. From a slight decrease in strength of magnetization to a complete disappearance of hysteresis loop has been observed in pure In_2O_3 thin films with increasing the annealing temperature from 250°C to 450°C , in the presence of air. The $(\text{In}_{1-x}\text{Ni}_x)_2\text{O}_3$ thin films annealed under vacuum follow a trend of enhancement in the strength of magnetization to increase in temperature from 250°C to 450°C . The hysteresis loop does not disappear at 450°C in $(\text{In}_{1-x}\text{Ni}_x)_2\text{O}_3$ thin films, as observed in the case of pure In_2O_3 thin films.

Keywords: Indium oxide; Thinfilms; Semiconductor, ferromagnetism

PACS Nos.: 75.70.-i; 75.47.Lx

1. Introduction

It is known that if the ferromagnetic property was attained in semiconductor by doping with suitable magnetic or non-magnetic ions into the host of non-magnetic

semiconductor, it is called as dilute magnetic semiconductor (DMS). Much attention is being put on these DMS materials which play an important role in magneto-optoelectronic devices or spintronics [1]. For the functional devices, the host semiconductor material, should possess the ferromagnetic property at room temperature [2]. Till today different magnetic and non-magnetic transition metal ions like chromium, iron, nickel, copper, etc., along with

*Corresponding author, E-mail: skaleemulla@gmail.com

non-transition metal ions like carbon, nitrogen, fluorine, were doped into the host semiconductors to generate ferromagnetism within the system. From the literature survey, it was found that the ferromagnetism in the materials was due to presence of impurity ions or defects [3–5]. Recent research on dilute magnetic oxides proved that even undoped oxide semiconductor thin films or nanoparticles of CeO_2 , In_2O_3 , ZnO , and TiO_2 exhibit ferromagnetism at room temperature [6–10]. It was suggested that point defects might be one of the possible reasons to attain ferromagnetism in these oxide semiconductors [11–13]. The origin of room temperature ferromagnetism in nanoparticles of above oxides has not been made clear. Among all the oxide semiconductors, the indium oxide (In_2O_3) is also an important material which finds its significance in many optoelectronic applications such as transparent conductors, flat panel displays, solar cells, gas sensors etc. The interesting properties of In_2O_3 include inheritance of wide band gap (3.5 eV), high carrier density, high transparency in the visible region and high electrical conductivity. The electrical conductivity of the In_2O_3 thin films can be tuned by controlling the stoichiometry of the films and/or doping with suitable metal ions [14]. If the films are dominated by indium, then they will exhibit high electrical conductivity with poor transparency. If the films are indium deficient, they will exhibit poor electrical conductivity with high optical transparency. Hence a proper control in the stoichiometry of the films is essential to maintain high electrical conductivity along with high optical transparency. When these In_2O_3 thin films were doped by small quantities of transition metal ions, they exhibited interesting magnetic properties which find new applications in the field of spintronics [15]. It is known that In_2O_3 is very sensitive to oxygen and thus oxygen vacancies will play an important role in changing the physical, chemical and magnetic properties of transition metal oxides [16]. The oxide semiconductors will exhibit Curie temperature above room temperature. Till now less research work has been carried out in understanding the intrinsic ferromagnetism of undoped indium oxide. The corresponding origin of intrinsic ferromagnetism and its underlying physics of this system are not yet made clear. In order to prove that the observed room temperature ferromagnetism is originating due to oxygen vacancies, the films have been annealed in air and in vacuum. The changes occurring in its magnetic properties due to different types of annealing have been studied systematically. It was found that the magnetic moment decreases with increasing the annealing temperature in the presence of air. It is also known that the magnetic moment depends directly on the number of oxygen vacancies created. So it is concluded from these facts that the formation of oxygen vacancies decreases with increasing the air annealing temperature. A detailed study

Fig. 1 (a) X-ray diffraction profiles of $(\text{In}_{1-x}\text{Ni}_x)_2\text{O}_3$ thin films at $x = 0.00$ annealed at various temperature. (b) X-ray diffraction profiles of $(\text{In}_{1-x}\text{Ni}_x)_2\text{O}_3$ thin films at $x = 0.03$ annealed at different temperatures. (c) X-ray diffraction profiles of $(\text{In}_{1-x}\text{Ni}_x)_2\text{O}_3$ thin films at $x = 0.05$ annealed at different temperatures and (d) X-ray diffraction profiles of $(\text{In}_{1-x}\text{Ni}_x)_2\text{O}_3$ thin films at $x = 0.07$ annealed at different temperatures. (e) X-ray diffraction profiles of $(\text{In}_{1-x}\text{Ni}_x)_2\text{O}_3$ thin films at $x = 0.05$, as deposited, air annealed and vacuum annealed at 250 °C

on the effect of air and vacuum annealing on structure, surface, optical and magnetic properties has been carried out and conclusions were being made as per the experimental results.

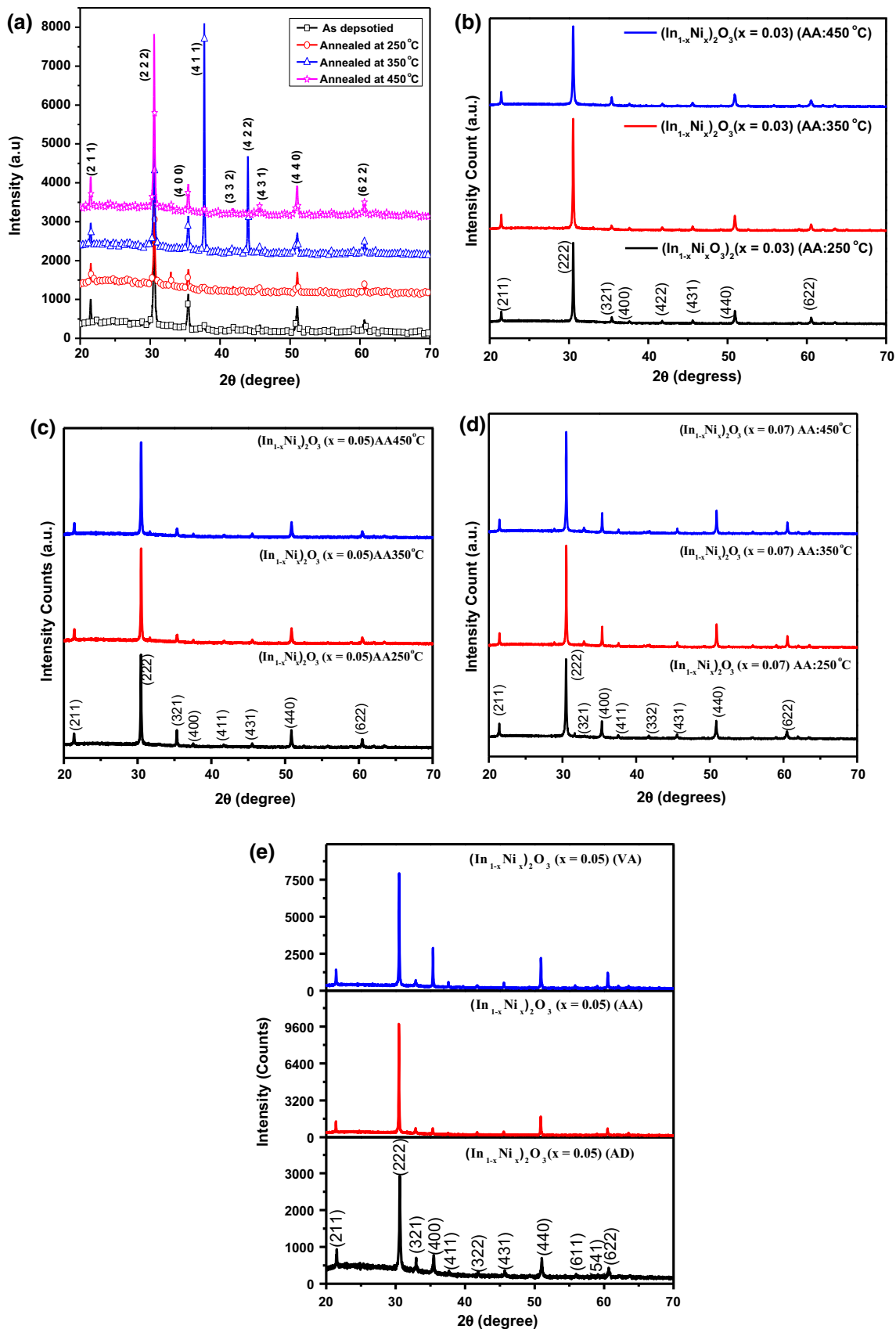
2. Experimental details

Nickel doped indium oxide thin films $(\text{In}_{1-x}\text{Ni}_x)_2\text{O}_3$ at $x = 0.00, 0.03, 0.05$ and 0.07 were prepared onto glass substrates by electron beam evaporation technique (12A4D). The source material for the films were taken as $(\text{In}_{1-x}\text{Ni}_x)_2\text{O}_3$ at $x = 0.00, 0.03, 0.05$ and 0.07 powders prepared by solid state reaction as discussed elsewhere [17]. Before coating, the glass substrates were cleaned following the general protocol. The substrates were mounted on the platform of resistive heaters. The substrate temperature was raised to 350 °C. A pressure of 1×10^{-6} mbar has been maintained during the film deposition. The thickness of the films was measured using in situ quartz crystal monitor. The thickness of about 150 nm was maintained for all the films. The crystal structures of the films were studied using X-ray diffractometer (D8 Advance, BRUKER). The morphology and chemical compositions of the films were studied using scanning electron microscope (SEM), energy dispersive analysis of X-rays (OXFORD instrument INCA penta FET X) and X-ray photo electron spectroscopy (K-Alpha, Thermo electron). The magnetic properties of the films were studied using vibrating sample magnetometer (Lake Shore 7404) at room temperature.

3. Results and discussion

3.1. Structural properties

Figure 1(a–d) show the X-ray diffraction (XRD) patterns of the $(\text{In}_{1-x}\text{Ni}_x)_2\text{O}_3$ thin films at different nickel doping concentrations. Figure 1(a) show the XRD profile of the $(\text{In}_{1-x}\text{Ni}_x)_2\text{O}_3$ thin film at $x = 0.00$. The diffraction peaks such as (2 1 1), (2 2 2), (4 0 0), (4 1 1), (3 3 2), (4 3 1), (4 4 0), (6 1 1), (5 4 1) and (6 2 2) were observed in the thin films. Between these diffraction planes, the (2 2 2) was



more predominant. No diffraction peaks related to unintentional impurities and secondary phases of indium/nickel were detected in the diffraction profiles within the detection limit of the XRD instrument. The intensity of the diffraction planes significantly improved with the rise of annealing temperature. There is an absence of shifting of diffraction peak position toward either lower or higher diffraction angle on increasing the annealing temperature. But the full width and half maxima decreased with increase of air annealing temperature.

Figure 1(b–d) indicate the X-ray diffraction profiles of $(\text{In}_{1-x}\text{Ni}_x)_2\text{O}_3$ thin films at different nickel doping concentrations. The crystallinity of the films has been found to increase with the rise of annealing temperature. In addition to this, a change in the diffraction angle towards the higher diffraction angles has been observed. This shift in diffraction angle is due to doping effect and not due to annealing. This is confirmed by the absence of shifting of any peaks for as deposited, air annealed and vacuum annealed $(\text{In}_{1-x}\text{Ni}_x)_2\text{O}_3$ thin films at $x = 0.05$ as shown in Fig. 1(e). No other diffraction peaks were observed in the films within the detection limit of the XRD instrument. However, In_2O_3 possess a high miscibility limit ($> 20\%$), so that no secondary peaks can be observed. Here, the XRD profiles of the NiO were also taken into the consideration to make sure that the observed ferromagnetism is not due to dopant element. No diffraction peak related to impurities of nickel in cluster form or nickel oxide formation was observed in the XRD profiles confirming the absence of the impurities in any form. A shift in diffraction peak towards higher angles has been observed in case of vacuum annealed $(\text{In}_{1-x}\text{Ni}_x)_2\text{O}_3$ at $x = 0.05$ thin films. Similar kinds of results were also noticed by Sun et al. [18] in pure In_2O_3 thin films prepared by sputtering technique.

3.2. Surface morphology

The surface morphology of the films was studied using field emission scanning electron microscope. Figure 2 shows the surface morphology of the $(\text{In}_{1-x}\text{Ni}_x)_2\text{O}_3$ thin films at $x = 0.07$, which has been as deposited and air annealed at different temperatures. From the SEM images, the grain size of the films was calculated and found to increase from 53 nm to 100 nm on increasing the annealing temperature. It may be due to the coalescence of small grains to form a bigger grain due to sufficient thermal energy. The $(\text{In}_{1-x}\text{Ni}_x)_2\text{O}_3$ thin films at $x = 0.00, 0.03$ and 0.05 follow the same surface morphology trend as $x = 0.07$. These kinds of results were also observed by Sudha et al. [19] in In_2O_3 thin films prepared by thermal evaporation technique.

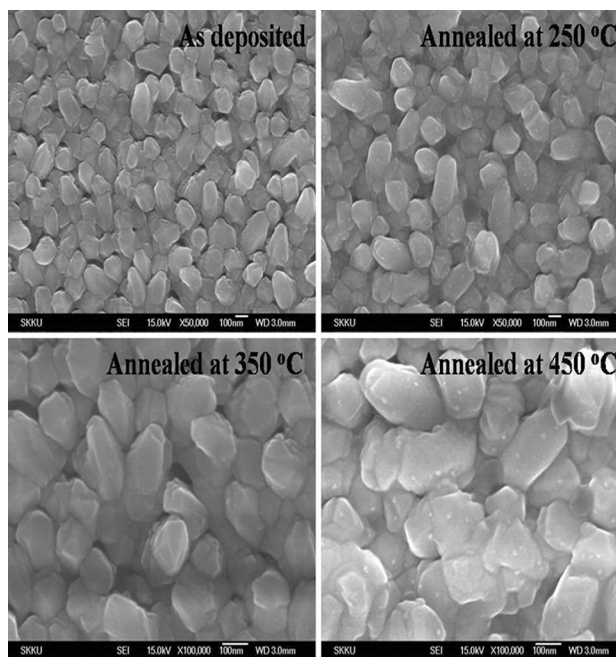


Fig. 2 The surface morphology of the $(\text{In}_{1-x}\text{Ni}_x)_2\text{O}_3$ thin films at $x = 0.07$ annealed at different temperatures

3.3. Compositional analysis

Figure 3 shows the EDAX spectrum of $(\text{In}_{1-x}\text{Ni}_x)_2\text{O}_3$ thin films at $x = 0.07$. Compositional studies were carried out for all the films at different doping concentrations of nickel. No new elements other than indium, nickel and oxygen were found to be present in the lattice indicating the absence of any dopant clusters in the matrix. Similar results were also found in $(\text{In}_{1-x}\text{Ni}_x)_2\text{O}_3$ thin films at different annealing temperatures. The valence states of indium, nickel and oxygen were studied using XPS spectroscopy. The elements such as In, Ni and O were present

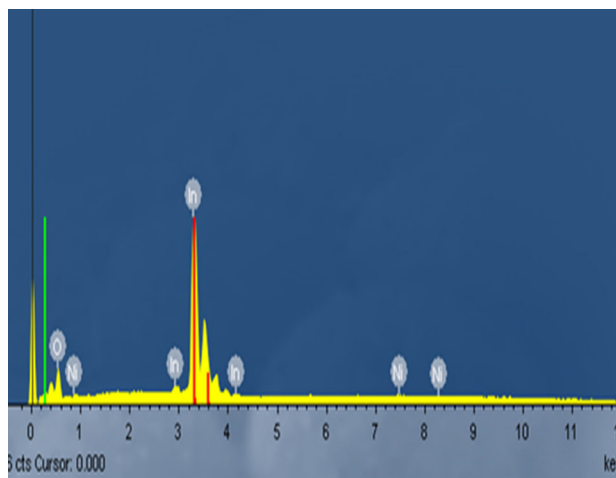


Fig. 3 EDAX spectrum of $(\text{In}_{1-x}\text{Ni}_x)_2\text{O}_3$ ($x = 0.07$) thin films annealed at $450\text{ }^\circ\text{C}$

at the desired binding energies. Figure 4(a–d) shows, XPS fine scans spectra of (a) In $3d$ edge, (b) Ni $2p$ edge and (c) O $1s$ edge spectra of the as deposited and vacuum annealed $(\text{In}_{1-x}\text{Ni}_x)_2\text{O}_3$ thin films at $x = 0.05$. Figure 4(a) shows the XPS spectrum of indium $3d$ edge. From the figure it can be seen that two major peaks were observed at 443.5 and 451 eV which represent the In $3d_{5/2}$ and In $3d_{3/2}$ states. These peaks are typical peaks of indium oxide phase [20]. The peaks at 444.2 eV and 451.8 eV represent the core levels of In $3d_{5/2}$ and In $3d_{3/2}$, respectively. A clear peak shift in binding energy had been observed for the as deposited and vacuum annealed films. Figure 4(b) shows the XPS spectrum of nickel $2p$ edge. A peak at 855 eV has been observed, which is the characteristic of Ni $2p_{3/2}$ [21]. Figure 4(c) shows the XPS spectrum of nickel O $1s$ edge. Two peaks at 529 eV and 531 eV were observed in this spectrum. These peaks shifted to higher binding energies with the increase of vacuum annealing temperature, which may be due to oxygen vacancies created in the films [22]. Figure 4(d) shows the

survey scan spectrum of as deposited and vacuum annealed $(\text{In}_{1-x}\text{Ni}_x)_2\text{O}_3$ thin films at 450 °C for $x = 0.05$. The elements indium, nickel and oxygen were present at their respective binding energies. So no new peaks related to any other impurities were found in the spectrum. The inset in the Fig. 4(c) showed the prominent indium prominent peak of as deposited and vacuum annealed thin films at 450 °C.

3.4. Optical properties

The optical transmittance and reflectance were recorded for $(\text{In}_{1-x}\text{Ni}_x)_2\text{O}_3$ thin films at $x = 0.03, 0.05$ and 0.07 annealed at different temperatures. An increase in optical transmittance has been observed with increase of air and vacuum annealing temperature [23]. The optical band gaps of the films were calculated using Tauc relation [24] depending on the type of transition for choosing constant A [25, 26].

Figure 5(a) shows the optical band gap of the $(\text{In}_{1-x}\text{Ni}_x)_2\text{O}_3$ thin films at $x = 0.03$ annealed at 250, 350 and

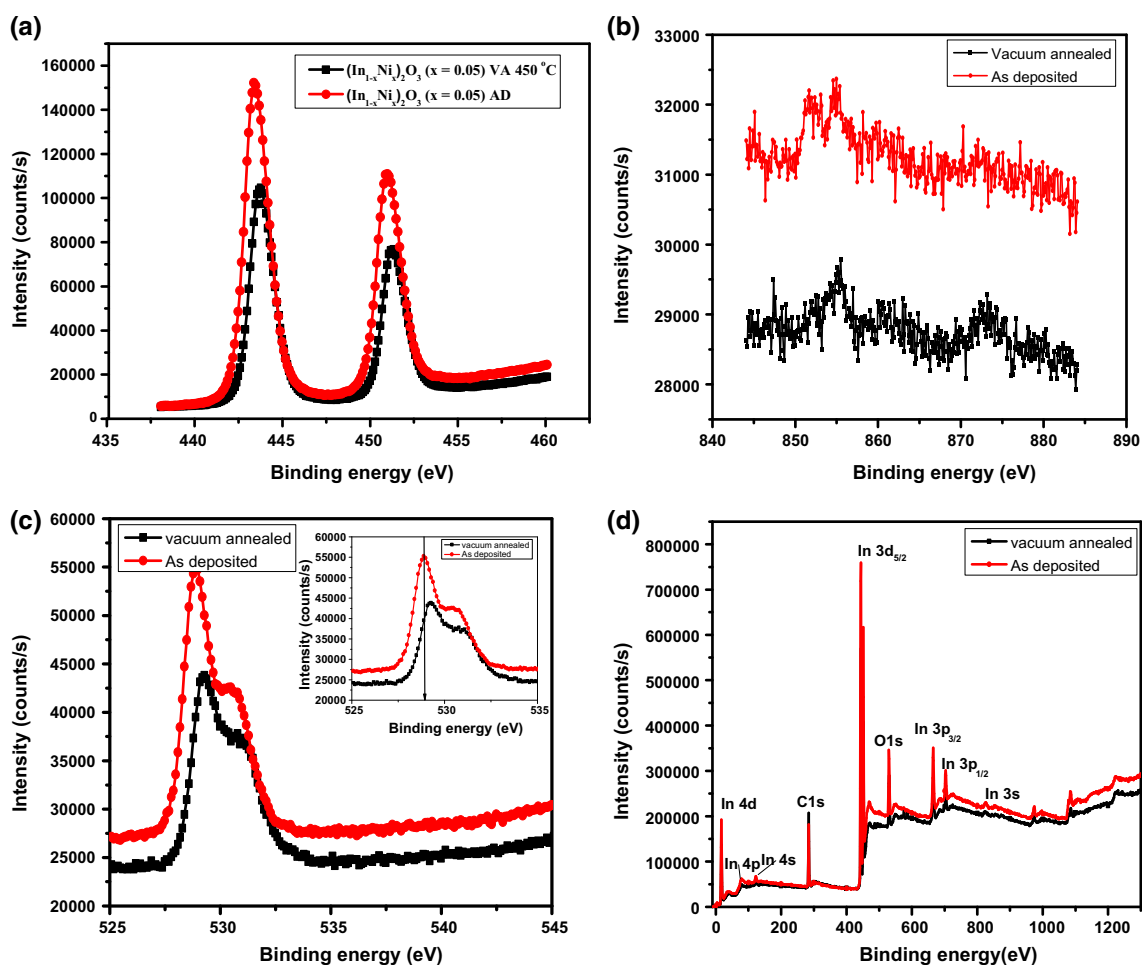


Fig. 4 XPS spectra of (a) Ni $2p$, (b) In $3d$, (c) O $1s$ and (d) survey spectrum of the as deposited and vacuum annealed $(\text{In}_{1-x}\text{Ni}_x)_2\text{O}_3$ thin film at $x = 0.05$

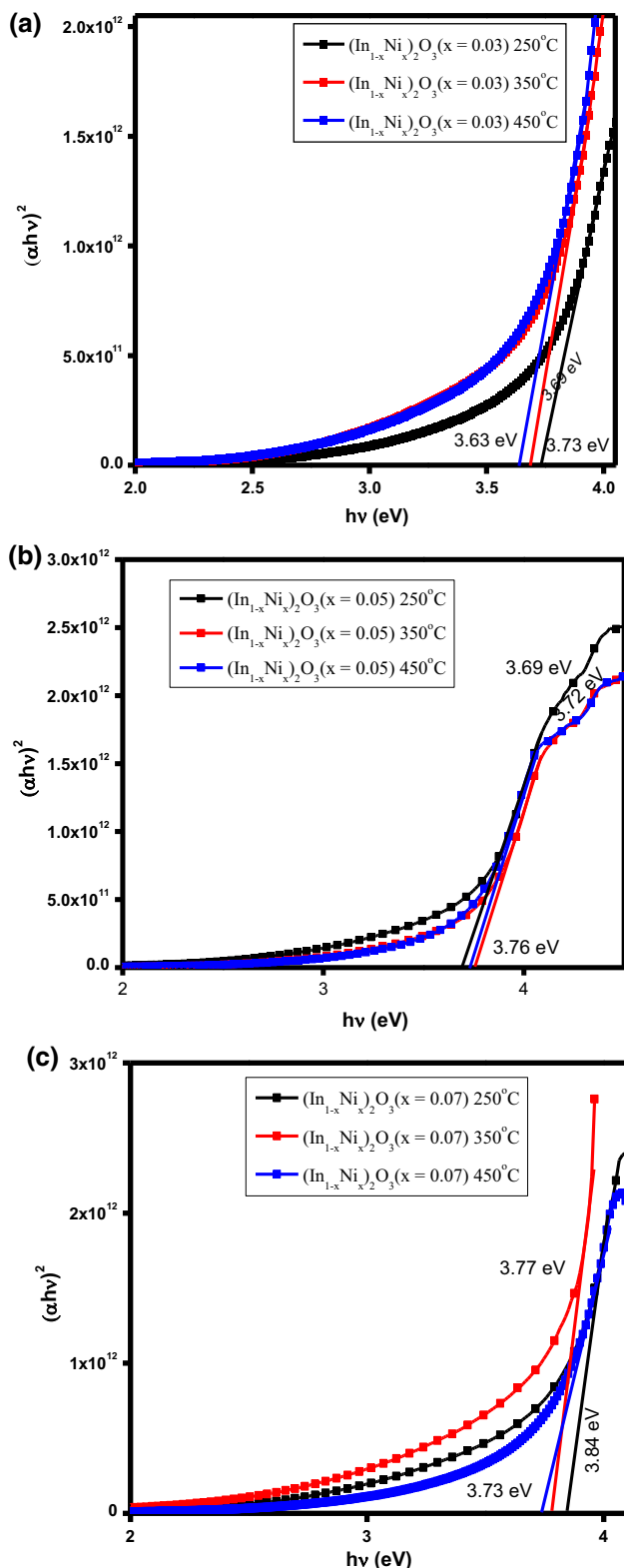


Fig. 5 Optical band gaps of $(\text{In}_{1-x}\text{Ni}_x)_2\text{O}_3$ thin films annealed at different temperatures (a) $x = 0.03$, (b) $x = 0.05$, (c) $x = 0.07$

450 °C, respectively. The band gap of the films decreased from 3.73 eV to 3.63 eV with increase of annealing

temperature from 250 °C to 450 °C. The same behavior was followed by $(\text{In}_{1-x}\text{Ni}_x)_2\text{O}_3$ thin films at $x = 0.05$ and 0.07 in which the band gap decreased from 3.76 eV to 3.69 eV and 3.84 eV to 3.73 eV, respectively with increase of air annealing temperature from 250 °C to 450 °C as shown in Fig. 5(b), (c). The observed band gaps in all the different annealing temperatures were consistent with that of the band gap of In_2O_3 thin films [27]. A decrease in optical band gap with an increase in annealing temperature was observed by Beena et al. [28] in laser ablated nano structured In_2O_3 thin films.

3.5. Magnetic properties

Figure 6(a) shows the M–H loops of the as deposited In_2O_3 thin films and also the In_2O_3 thin films annealed in air at different temperatures. The as deposited and air annealed thin films exhibited ferromagnetism at room temperature. The strength of magnetization increased with the increase of the applied field and became saturated at higher magnetic fields. The as deposited In_2O_3 thin films have shown the saturation magnetization of 23.2 emu/cm³. The saturation magnetization for In_2O_3 thin films annealed at different temperature has been found to decrease slightly with increasing the air annealing temperature. The magnetic hysteresis in pure In_2O_3 may come from the defects such as oxygen vacancies. The undoped In_2O_3 in bulk form has shown diamagnetism where as in thin film forms it showed ferromagnetism at room temperature. It is suggested that the oxygen vacancies created during preparation of the films might be one of the possible reasons for the observed room temperature ferromagnetism. The films annealed at 350 °C showed the magnetization value 20 emu/cm³. The decrease in the magnetization with an increase of annealing temperature might be due to decrease in oxygen vacancies. The ferromagnetic nature completely disappeared and the films became diamagnetic when the films were annealed at 450 °C as shown in Fig. 6(b). Hence, in this investigation different magnetic states such as diamagnetism and weak ferromagnetism were observed in In_2O_3 thin films. The hysteresis loop completely disappeared when the films were air annealed at 450 °C. It may be due to filling of oxygen deficiencies when annealed in air or oxygen environment. Hence the In_2O_3 thin films annealed in the presence of air at 450 °C exhibits the stoichiometry of bulk In_2O_3 responsible for diamagnetism at room temperature. Hence different magnetic states have been observed in the present study. Further, ferromagnetism was observed in undoped indium oxide thin films when the films were annealed under oxygen deficient environment in vacuum [18, 29–31]. In the case of undoped In_2O_3 , neither In^{3+} nor O^{2-} is magnetic in nature leading to absence of ferromagnetism. As it is known, oxygen vacancies can be easily

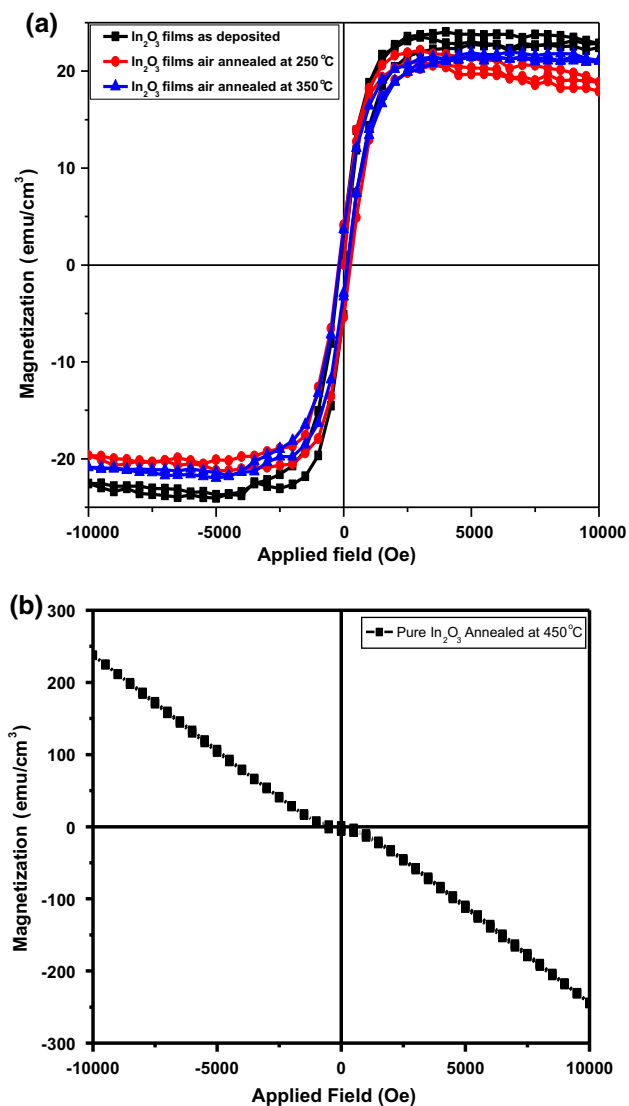


Fig. 6 (a) M–H loop of the $(\text{In}_{1-x}\text{Ni}_x)_2\text{O}_3$ thin films at $x = 0.00$ annealed at 250 °C and 350 °C. (b) M–H loop of the $(\text{In}_{1-x}\text{Ni}_x)_2\text{O}_3$ thin films at $x = 0.00$ annealed at 450 °C

created in In_2O_3 [32]. It is just these oxygen vacancies that are widely thought to be related to the origin of ferromagnetism in In_2O_3 as well as in other oxide based DMS systems. Ferromagnetism was reported in pure In_2O_3 and other oxide semiconductor thin films with high oxygen vacancy concentrations [33].

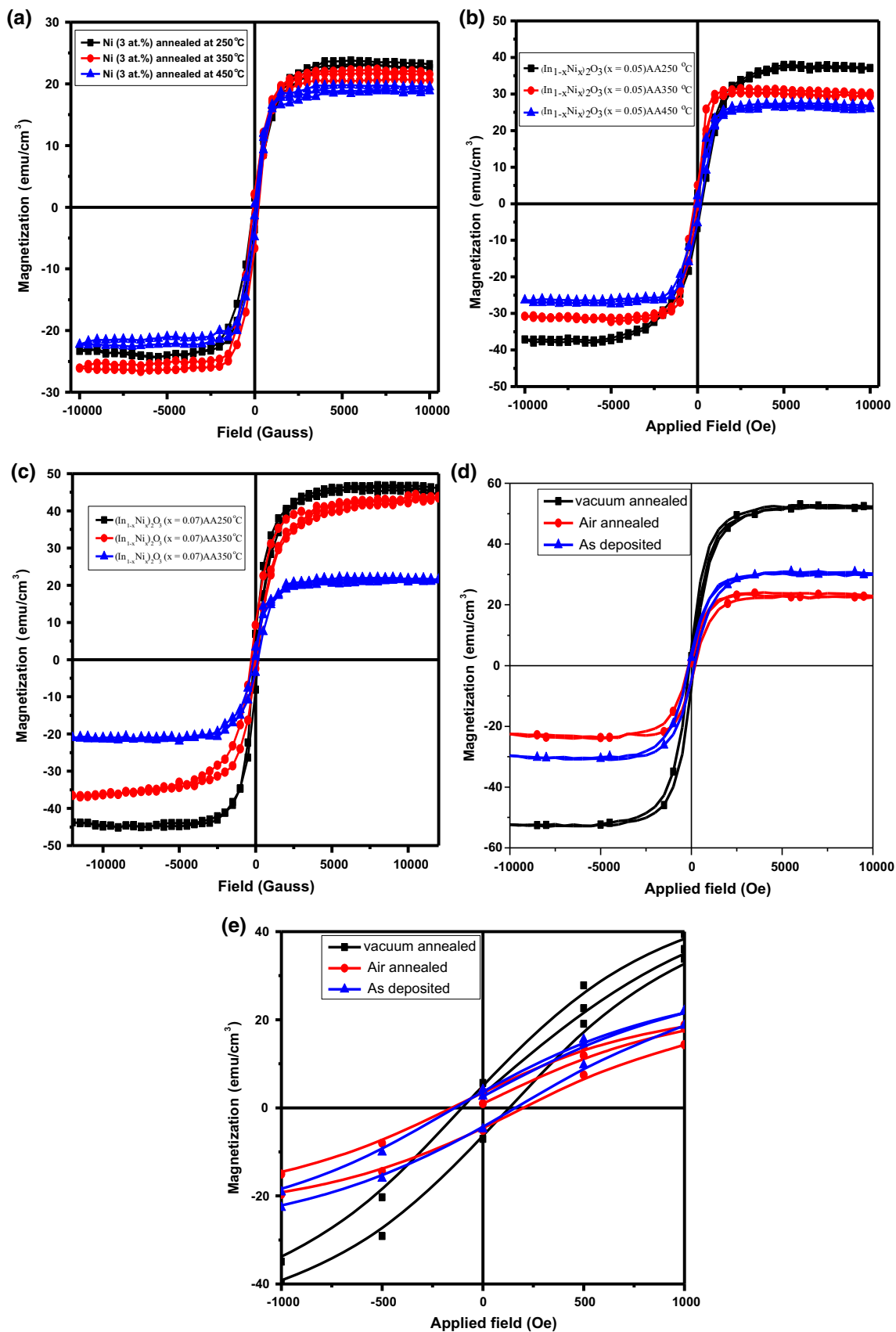
In order to study the role of air annealing temperature on the magnetic properties of impurity doped oxide semiconductor, nickel doped indium oxide thin films $(\text{In}_{1-x}\text{Ni}_x)_2\text{O}_3$ at different Ni doping concentrations were also annealed in air at 250 °C, 350 °C and 450 °C. The studies reflect that the observed ferromagnetism in $(\text{In}_{1-x}\text{Ni}_x)_2\text{O}_3$ is not extrinsic in nature as no evidence of impurity element has been detected in XRD. Figure 7(a) shows the M–H loop of $(\text{In}_{1-x}\text{Ni}_x)_2\text{O}_3$ thin films at $x = 0.03$ annealed at

different temperatures. Here very small variation in the magnetic moment of the films has been observed with an increase of annealing temperature. The as deposited films exhibited the magnetic moment 22.94 emu/cm³ whereas the films annealed at 450 °C exhibited 18 emu/cm³.

Figure 7(a–c) show the M–H curves of the $(\text{In}_{1-x}\text{Ni}_x)_2\text{O}_3$ thin films at $x = 0.03, 0.05$ and 0.07 annealed at different temperatures. In the $(\text{In}_{1-x}\text{Ni}_x)_2\text{O}_3$ thin films the induced ferromagnetism could be due to oxygen vacancies and/or Ni dopant ions. To elucidate the source of ferromagnetism and role of oxygen vacancies, we have annealed all the samples at 250 °C, 350 °C and 450 °C. From the above figures, it is clear that the saturation magnetic moment increased with increase of Ni doping concentration, whereas the same decreased with increase of air annealing temperature. The saturation magnetic moment of the samples decreased noticeably with the increase of the annealing temperature at higher concentration. Even the Ni doped In_2O_3 samples annealed at 450 °C showed ferromagnetic nature with the significant saturation magnetic moment. This indicates that the ferromagnetism is induced by both oxygen vacancies as well as nickel dopants. However, the contribution of oxygen vacancies could be completely eliminated by annealing the samples at 450 °C. Thus the saturation magnetic moment attained at 450 °C annealed samples could only be due to Ni dopants. This conclusion was arrived by the fact that the undoped In_2O_3 thin film annealed at 450 °C showed magnetic property of bulk In_2O_3 (diamagnetic).

Hence, in this study it is concluded that the oxygen environment strongly affects the room temperature ferromagnetism. The origin of the different magnetic states was explained in our earlier reports [34–36]. During annealing these vacancies are filled with oxygen and hence leads to decrease in the oxygen deficiency in In_2O_3 film. This leads to decrease of ferromagnetism with a decrease in oxygen vacancies [37]. Hence it is suggested that air annealing reduces the oxygen deficiencies. But when films were annealed in a vacuum, they did not bring drastic change in magnetization. Hence it is proved that the decrease in oxygen vacancies could reduce the ferromagnetic order in thin films.

As a result, the annealing causes dramatic degradation in the number of oxygen deficiencies. It is clearly evident that the source of ferromagnetism in these systems might well originate from creation of oxygen vacancies. The connection between the highly oxygen-deficiency states and the enhanced ferromagnetism indicates that oxygen vacancies play a crucial role in mediating the d^0 ferromagnetism in the pure In_2O_3 films [38]. Hence in this investigation, different magnetic states such as diamagnetism in bulk form and weak ferromagnetism in the annealed undoped In_2O_3 thin films were observed.



◀**Fig. 7** (a) M–H curves of $(\text{In}_{1-x}\text{Ni}_x)_2\text{O}_3$ thin films at $x = 0.03$ annealed at different temperatures, (b) M–H curves of $(\text{In}_{1-x}\text{Ni}_x)_2\text{O}_3$ thin films at $x = 0.05$ annealed at different temperatures and (c) M–H curves of $(\text{In}_{1-x}\text{Ni}_x)_2\text{O}_3$ thin films at $x = 0.07$ annealed at different temperatures. (d) M–H curves of as deposited, annealed and vacuum annealed $(\text{In}_{1-x}\text{Ni}_x)_2\text{O}_3$ thin films at $x = 0.05$. (e) M–H loops of as deposited, annealed and vacuum annealed $(\text{In}_{1-x}\text{Ni}_x)_2\text{O}_3$ thin films at $x = 0.05$ in the applied field range of -1000 to $+1000$ Oe

Table 1 Summary of saturation magnetization of the films with different composition, air annealing and vacuum annealing (VA) temperatures

	AD (emu/ cm^3)	250 °C (emu/ cm^3)	350 °C (emu/ cm^3)	450 °C (emu/ cm^3)	450 °C (VA) (emu/ cm^3)
$x = 0.00$	23.2	20.6	21.7	Dia	–
$x = 0.03$	22.94	23	22	19	–
$x = 0.05$	31.39	37	29	25	53.81
$x = 0.07$	27.82	46	42	20	–

Figure 7(d), (e) shows the M–H loop of the $(\text{In}_{1-x}\text{Ni}_x)_2\text{O}_3$ thin films at $x = 0.05$ which were as deposited, air annealed and vacuum annealed at 450 °C under applied magnetic field of ± 10 kOe and ± 1 kOe respectively. From the figure it has been evident that the saturation magnetizations of the air annealed films were found to decrease whereas the strength of the magnetization increased in case of vacuum annealing. All the films exhibited ferromagnetism at room temperature with weak magnetic hysteresis loop in pure In_2O_3 . The saturation magnetization increased in Ni doped In_2O_3 thin film from 31.39 to 53.81 emu/cm^3 when the samples were annealed at 450 °C under vacuum. The magnetic polarons were formed due to oxygen vacancies along with trapped electrons in the Ni doped In_2O_3 leading to the origination of the room temperature ferromagnetism in nickel doped In_2O_3 thin films. The vacuum annealing process could achieve more oxygen vacancies in the Ni doped In_2O_3 , which causes the high ferromagnetism in the system. The behavior of varying strength of ferromagnetism under alternate annealing processes and their strong relationship with the oxygen vacancies is a convincing evidence to conclude that the ferromagnetism in $(\text{In}_{1-x}\text{Ni}_x)_2\text{O}_3$ thin film at $x = 0.05$ can be directly controlled by oxygen vacancies. This behavior was also observed by Singhal et al. [39] in Fe doped In_2O_3 thin films when the films were annealed in different ambiances. The magnetization of films with annealing temperature is shown in Table 1.

4. Conclusions

$(\text{In}_{1-x}\text{Ni}_x)_2\text{O}_3$ ($x = 0.03, 0.05$ and 0.07) thin films were prepared using the electron beam evaporation technique and subjected to air and vacuum annealing. All the films were body centered cubic in structure with no impurities. The crystallite size increased with increase of air and vacuum annealing temperature. The optical band gap of the films decreased with increase of air annealing temperature. All the films were ferromagnetic at room temperature and the strength of magnetization decreased with increase of air annealing temperature and the undoped indium oxide films became diamagnetic at 450 °C. The Ni doped films were ferromagnetic and the strength of magnetization decreased with increasing annealing temperature, but the magnetization remained in the films even at a higher air annealing temperatures. The strength of magnetization increased with increase of vacuum annealing temperature. This concludes that the observed ferromagnetism originates due to its intrinsic property rather than due to the presence of any other impurities.

Acknowledgements Authors are grateful to UGC-DAE-CSR, IGCAR, Kalpakkam, 603102, Tamil Nadu, India for providing financial support under Project Sanction Number (CSR-KN/CRS-72/2015-2016/809) to carry out the present work. The authors are highly thankful to VIT-SIF for providing, XRD, SEM and DRS facilities to carry out the present work.

References

- [1] C Guglieri and J Chaboy *J. Phys. Chem. C* **114** 19629 (2010)
- [2] Q Wang, Q Sun, G Chen, Y Kawazoe and P Jena *Phys. Rev. B* **77** 205411 (2008)
- [3] A K Das and A Srinivasan *J. Magn. Magn. Mater.* **404** 190 (2016)
- [4] N H Hong, J Sakai and F Gervais *J. Magn. Magn. Mater.* **316** 214 (2007)
- [5] J Li, G Bai, Y Jiang, Y Du, C Wu and M Yan *J. Magn. Magn. Mater.* **426** 545 (2017)
- [6] D Bérardan, E Guilmeau and D Pelloquin *J. Magn. Magn. Mater.* **320** 983 (2008)
- [7] P Hajra, P Brahma, S Dutta, S Banerjee and D Chakravorty *J. Magn. Magn. Mater.* **324** 1425 (2012)
- [8] K Nadeem, A Ullah, M Mushtaq, M Kamran, S S Hussain and M Mumtaz *J. Magn. Magn. Mater.* **417** 6 (2016)
- [9] H Qin, Z Zhang, X Liu, Y Zhang and J Hu *J. Magn. Magn. Mater.* **322** 1994 (2010)
- [10] J Stankiewicz, F Villuendas, J Bartolomé and J Sesé *J. Magn. Magn. Mater.* **310** 2084 (2007)
- [11] A M A Hakeem *J. Magn. Magn. Mater.* **322** 709 (2010)
- [12] N H Hong *J. Magn. Magn. Mater.* **303** 338 (2006)
- [13] P Mohanty, D Kabiraj, R K Mandal, P K Kulriya, A S K Sinha and C Rath *J. Magn. Magn. Mater.* **355** 240 (2014)
- [14] J R Bellingham, A P Mackenzie and W A Phillips *Appl. Phys. Lett.* **58** 2506 (1991)
- [15] M Venkatesan, C B Fitzgerald, J G Lunney and J M D Coey *Phys. Rev. Lett.* **93** 177206 (2004)

- [16] E Wahlström, E K Vestergaard, R Schaub, A Rønnau, M Vestergaard, E Lægsgaard, I Stensgaard and F Besenbacher *Science* **303** 511 (2004)
- [17] N S Krishna, S Kaleemulla, G Amarendra, N M Rao, M Kuppan, M R Begam and D S Reddy *Mater. Sci. Semicond. Process.* **18** 22 (2014)
- [18] S Sun, P Wu and P Xing *Appl. Phys. Lett.* **101** 132417 (2012)
- [19] A Sudha, S L Sharma and T K Maity *Mater. Lett.* **157** 19 (2015)
- [20] Z Fanhao, X Zhang, W Jin, W Lisheng and Z Lina *Nanotechnology* **15** 596 (2004)
- [21] M C Biesinger, B P Payne, A P Grosvenor, L W M Lau, A R Gerson and R S C Smart *Appl. Surf. Sci.* **257** 2717 (2011)
- [22] S Sharma, S Chaudhary, S C Kashyap and S K Sharma *J. Appl. Phys.* **109** 083905 (2011)
- [23] A S A C Diniz and C J Kiely *Renew. Energy* **29** 2037 (2004)
- [24] J Tauc *Amorphous and Liquid Semiconductors* (ed.) J Tauc (New York, NY, USA: Plenum Press) p 159 (1974)
- [25] K J Lethy, D Beena, R V Kumar, V P M Pillai, V Ganesan and V Sathe *Appl. Surf. Sci.* **254** 2369 (2008)
- [26] J R Rani, V P M Pillai, R S Ajimsha, M K Jayaraj and R S Jayasree *J. Appl. Phys.* **100** 014302 (2006)
- [27] D Liu, W Lei, B Zou, S Yu, J Hao, K Wang, B Liu, Q Cui and G Zou *J. Appl. Phys.* **104** 083506 (2008)
- [28] D Beena, K J Lethy, R Vinodkumar, A P Detty, V P M Pillai and V Ganesan *J. Alloys Compd.* **489** 215 (2010)
- [29] S A Ahmed *J. Magn. Magn. Mater.* **402** 178 (2016)
- [30] B Kisan, P Saravanan, S Layek, H C Verma, D Hesp, V Dhanak, S Krishnamurthy and A Perumal *J. Magn. Magn. Mater.* **384** 296 (2015)
- [31] C Sudakar, P Kharel, R Suryanarayanan, J S Thakur, V M Naik, R Naik and G Lawes *J. Magn. Magn. Mater.* **320** L31 (2008)
- [32] H L Hartangel, A L Daar, A K Jain and C Jagadish *Semiconducting Transparent Thin Films* (ed.) H L Hartangel (Bristol, Philadelphia: Taylor & Francis) p 14 (1995)
- [33] N H Hong, J Sakai, N Poirot and V Brizé *Phys. Rev. B* **73** 132404 (2006)
- [34] S H Babu, S Kaleemulla, N M Rao and C Krishnamoorthi *J. Electron. Mater.* **45** 5703 (2016)
- [35] M Kuppan, S Kaleemulla, N M Rao, C Krishnamoorthi, G V Rao, I Omkaram and D S Reddy *J. Supercond. Nov. Magn.* **30** 981 (2017)
- [36] M Kuppan, S Kaleemulla, N M Rao, C Krishnamoorthi, I Omkaram and D S Reddy *J. Mater. Sci. Mater. Electron.* **28** 2976 (2017)
- [37] Q Y Wen, H W Zhang, Q H Yang, Y Q Song and J Q Xiao *J. Magn. Magn. Mater.* **321** 3110 (2009)
- [38] L M Huang, C M Araújo and R Ahuja *Eur. Phys. Lett.* **87** 27013 (2009)
- [39] R K Singhal, A Samariya, S Kumar, S C Sharma, Y T Xing, U P Deshpande, T Shripathi and E Saitovitch *Appl. Surf. Sci.* **257** 1053 (2010)